

Quantitative Determination of Eliashberg Function and Evidence of Strong Electron Coupling with Multiple Phonon Modes in Heavily Over-doped $(\text{Bi,Pb})_2\text{Sr}_2\text{CuO}_{6+\delta}$

Lin Zhao¹, Jing Wang², Junren Shi^{2,*}, Wentao Zhang¹, Haiyun Liu¹, Jianqiao Meng¹, Guodong Liu¹, Xiaoli Dong¹, Wei Lu¹, Guiling Wang³, Yong Zhu³, Xiaoyang Wang³, Qinjun Peng³, Zhimin Wang³, Shenjin Zhang³, Feng Yang³, Chuangtian Chen³, Zuyan Xu³, and X. J. Zhou^{1,†}

¹*National Lab for Superconductivity, Beijing National Laboratory for Condensed Matter Physics, Institute of Physics, Chinese Academy of Science, Beijing 100190, China*

²*Beijing National Laboratory for Condensed Matter Physics,*

Institute of Physics, Chinese Academy of Science, Beijing 100190, China

³*Technical Institute of Physics and Chemistry, Chinese Academy of Sciences, Beijing 100190, China*

(Dated: January 31, 2010)

Super-high resolution laser-based angle-resolved photoemission spectroscopy measurements have been carried out on a heavily overdoped $(\text{Bi,Pb})_2\text{Sr}_2\text{CuO}_{6+\delta}$ ($T_c \sim 5$ K) superconductor. Taking advantage of the high-precision data on the subtle change of the quasi-particle dispersion at different temperatures, we develop a general procedure to determine the bare band dispersion and extract the bosonic spectral function quantitatively. Our results show unambiguously that the ~ 70 meV nodal kink is due to the electron coupling with the multiple phonon modes, with a large mass enhancement factor $\lambda \sim 0.42$ even in the heavily over-doped regime.

PACS numbers: 74.25.Jb, 71.38.-k, 74.72.Gh, 79.60.-i

The interaction of electrons with phonons and other collective excitations (bosons) in solids dictates fundamental physical properties of materials [1]. In a Fermi liquid picture, such interaction can be described by the Eliashberg spectral function $\alpha^2 F(\omega)$, which accounts for the bosonic modes involved in the coupling and their strengths. In the conventional superconductors, extraction of the Eliashberg function played a key role in pinning down the phonon as the glue for the electron pairing that gives rise to the BCS superconductivity [2]. For high temperature cuprate superconductors and other complex compounds, one expects that the extraction of the Eliashberg function will also be important in understanding the exotic physical properties and the mechanism of high temperature superconductivity [3–8].

The electron-boson coupling gives rise to the band renormalization and the change of the quasiparticle scattering rate, which can be described by the real part ($\text{Re}\Sigma(k, \omega)$) and the imaginary part ($\text{Im}\Sigma(k, \omega)$) of the electron self-energy $\Sigma(k, \omega)$, respectively. With the dramatic improvement of resolution, angle-resolved photoemission spectroscopy (ARPES) has emerged as a powerful tool in probing such many-body effects [5]. Under the sudden approximation, it measures the single particle spectral function $A(k, \omega) = (1/\pi)\text{Im}\Sigma(k, \omega)/\{[\omega - \epsilon_k^0 - \text{Re}\Sigma(k, \omega)]^2 + [\text{Im}\Sigma(k, \omega)]^2\}$, which is directly related to the electron self-energy [5]. ARPES has been extensively employed in investigating many-body effects in conventional metals [9, 10], graphene [11] and complex materials [5, 12]. However, a long-standing issue with the ARPES technique is the ambiguous “bare band” ϵ_k^0 [13], which hinders a quantitative determination of the electron self-energy $\text{Re}\Sigma(k, \epsilon) = \epsilon - \epsilon_k^0$ and the underlying bosonic spectral function $\alpha^2 F(\omega)$ [6–8].

Coming specifically to high- T_c cuprate superconductors, although there is a general consensus on the electron-boson coupling as the origin of the universally observed 50~80 meV dispersion kink along the $(0,0)$ - (π, π) nodal direction [14–20], it remains under debate on the nature of the boson(s) involved, mainly between phonons [15] and magnetic origins [19, 21, 22]. Theoretical calculations suggest that the electron-phonon coupling in cuprates is too weak to account for the nodal kink [23, 24]. To eventually resolve the issue, it is crucial to extract the bosonic spectral function quantitatively so that a direct comparison between the experiments and the calculations could be possible [6–8].

In this paper, we introduce a new approach which can unambiguously determine the bare quasi-particle dispersion, and hence enables the quantitative determination of the bosonic spectral function. The method utilizes the subtle change of the quasi-particle dispersion induced by the temperature. This is made possible by the super-high resolution laser-based ARPES measurements, which present data of the significantly higher quality feasible for a quantitative analysis of a modified maximum entropy method [6]. By carrying out such a procedure on a heavily over-doped $(\text{Bi,Pb})_2\text{Sr}_2\text{CuO}_{6+\delta}$ (Pb-Bi2201, $T_c \sim 5$ K), we are able to determine the bare band and extract the bosonic spectral function quantitatively along the nodal direction. Our results present a conclusive evidence that the electron-boson coupling is strong (with a mass enhancement factor $\lambda \approx 0.42$) even in the heavily over-doped cuprate compounds, and it originates from the electron coupling to the multiple phonon modes. Moreover, our approach is general enough to be applicable for many other materials.

The angle-resolved photoemission measurements have

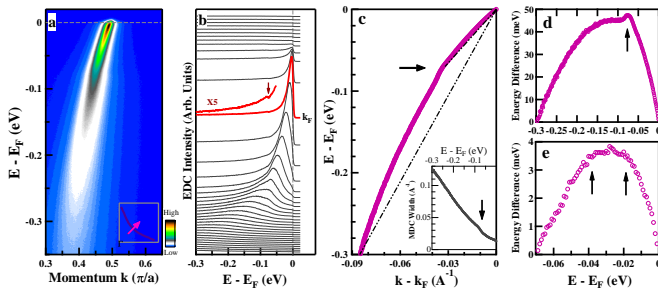


FIG. 1: Fine structure in the nodal dispersion of a heavily over-doped Pb-Bi2201 ($T_c \sim 5$ K) measured at 15 K. (a) Photoemission image taken along the $(0,0)-(\pi,\pi)$ nodal direction with the location of the momentum cut shown in the inset. (b) Corresponding photoemission spectra (energy distribution curves, EDCs). The EDC at the Fermi momentum k_F (red curve) shows a dip feature at ~ 73 meV, as indicated by an arrow in the expanded spectrum. (c) Quasi-particle dispersion obtained by fitting MDCs (momentum distribution curves) at different binding energies. The inset shows the corresponding MDC width (FWHM). (d) Energy difference between the measured dispersion and a straight line connecting 0 (E_F) and -0.3 eV. A peak at ~ 73 meV is clearly observed as indicated by an arrow. (e) Energy difference between the measured dispersion and a straight line connecting 0 and -0.07 eV. Two features can be identified at ~ 41 meV and ~ 17 meV.

been carried out on our newly developed vacuum ultraviolet (VUV) laser-based ARPES system [25]. The photon energy of the laser is 6.994 eV with a bandwidth of 0.26 meV. The overall instrumental energy resolution is set at 1 meV, which is significantly improved from 10~20 meV of previous measurements [6–8, 14–20]. The angular resolution is ~ 0.3 degree, corresponding to a momentum resolution $\sim 0.004 \text{ \AA}^{-1}$ at the photon energy of 6.994 eV, more than twice improved from 0.009 \AA^{-1} at a usual photon energy of 21.2 eV for the same angular resolution. The heavily overdoped $(\text{Bi,Pb})_2\text{Sr}_2\text{CuO}_{6+\delta}$ (Pb-Bi2201) single crystals with a $T_c \sim 5$ K were grown by the traveling-solvent floating zone method. The samples are cleaved *in situ* in vacuum with a base pressure better than 5×10^{-11} Torr.

Figure 1(a) shows the raw data of photoemission image taken on a heavily overdoped Pb-Bi2201 ($T_c \sim 5$ K) sample along the $(0,0)-(\pi,\pi)$ nodal direction at 15 K. Clear kink is observed near 70 meV in the dispersion extracted from MDC (momentum distribution curve) fitting (Fig. 1(c)), with a corresponding drop in the MDC width (inset of Fig. 1(c)). In order to reveal the possible fine structures in the dispersion, we plot the energy difference between the measured dispersion and a featureless straight line connecting 0 (E_F) and -0.3 eV on the dispersion (Fig. 1(d)). A prominent peak shows up near ~ 73 meV. In addition, in the energy difference between the measured dispersion and another straight line connecting 0 and -0.07 eV (Fig. 1e), one can also identify

low energy features at ~ 41 meV and ~ 17 meV, signified by the slope changes. We note that these three features at ~ 73 meV, ~ 41 meV, and ~ 17 meV are robust and have been reproduced in several independent measurements. Moreover, a clear dip at 73 meV (Fig. 1(b)) can be observed on the EDCs (energy distribution curves) near the Fermi momentum (k_F).

The underlying bosonic spectral function $\alpha^2 F(\omega)$ can be extracted from the measured real part of the electron self-energy [6]. The real part of self-energy is related to $\alpha^2 F(\omega)$ by:

$$\text{Re}\Sigma(\epsilon; T) = \int_0^\infty d\omega K\left(\frac{\epsilon}{kT}, \frac{\omega}{kT}\right) \alpha^2 F(\omega), \quad (1)$$

where $K(y, y') = \int_{-\infty}^\infty dx f(x-y)2y'/(x^2-y'^2)$ with $f(x)$ being the Fermi distribution function [1]. In the ARPES measurements, the real part of the electron self-energy is determined from the measured MDC dispersion ϵ_k by $\text{Re}\Sigma(\epsilon_k) = \epsilon_k - \epsilon_k^0$, where ϵ_k^0 is the bare quasi-particle dispersion for an *ad-hoc* system with the electron-boson coupling turned off [26]. Attempts have been made to invert the “effective” bosonic spectral function $\alpha^2 F(\omega)$ from the measured MDC dispersion by assuming an empirical bare band of a quadratic form $\epsilon_k^0 = a(k-k_F)^2 + b(k-k_F)$ [6–8]. It was found that the qualitative features of the bosonic spectral function do not sensitively depend on the choice of the bare band. However, the arbitrariness

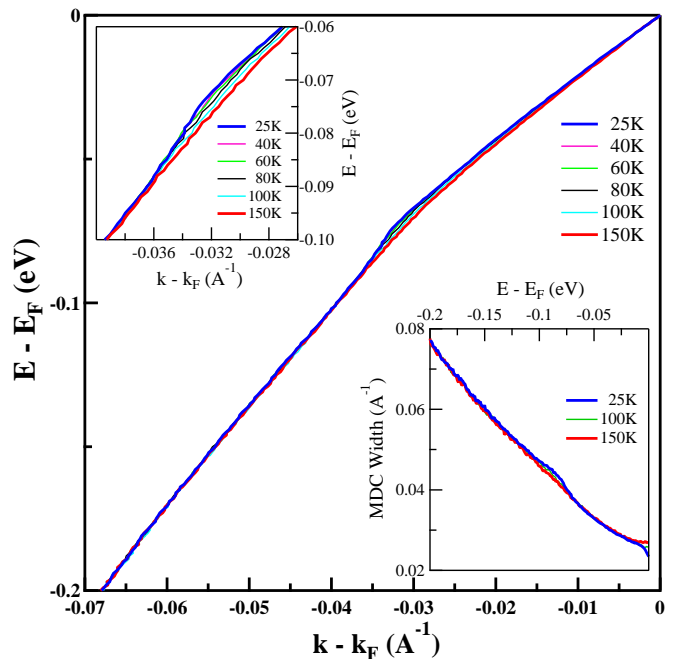


FIG. 2: Temperature dependence of the nodal dispersion measured on a heavily over-doped Pb-Bi2201 ($T_c \sim 5$ K). The dispersions near the kink region are expanded in the up-left inset. The bottom-right inset shows MDC width measured at 25 K, 100 K and 150K.

in choosing the appropriate parameters for the bare band prevents a quantitative determination of the bosonic spectral function [6–8]. Here we propose a general approach to circumvent this problem by making use of the self-energy change at different temperatures. We assume that $\alpha^2 F(\omega)$ and the bare band have negligible temperature dependence over a relatively small temperature window, and the Eliashberg function can be extracted from the self-energy difference at different temperatures by:

$$\begin{aligned} \text{Re}\Sigma(\epsilon; T_1) - \text{Re}\Sigma(\epsilon; T_2) &= \int_0^\infty d\omega \alpha^2 F(\omega) \\ &\times \left[K\left(\frac{\epsilon}{kT_1}, \frac{\omega}{kT_1}\right) - K\left(\frac{\epsilon}{kT_2}, \frac{\omega}{kT_2}\right) \right] \quad (2) \end{aligned}$$

The successful application of the approach relies critically on the high quality of data, as it utilizes a small temperature-induced change between two dispersions subjected to noises. Such a stringent requirement on the data quality can now be met by the super-high resolution laser-ARPES measurements (Fig. 2). In this paper, we test our new approach on the heavily overdoped Pb-Bi2201, in which the electron-electron correlation is relatively weak, and Eq. (2) is believed to be applicable.

Figure 3 shows the detailed procedure to extract the bare band dispersion and the bosonic spectral function. To obtain the bosonic spectral function $\alpha^2 F(\omega)$ from Eq. (2), one needs to know the difference of the real part of self-energy $\Delta \text{Re}\Sigma(\epsilon) \equiv \text{Re}\Sigma(\epsilon; T_1) - \text{Re}\Sigma(\epsilon; T_2)$ at two different temperatures, as schematically shown in Fig. 3(a). Here, we use two dispersions measured at 25 K and 100 K. Note that $\Delta \text{Re}\Sigma(\epsilon)$ depends on the selection of the bare band dispersion. As the result, an iteration approach is needed, as detailed in the following: (1) Determine $\Delta \text{Re}\Sigma(\epsilon)$ based on the current selection of the bare band dispersion. The initial value ($\Delta \text{Re}\Sigma_0(\epsilon)$) is taken as the direct difference between the two dispersions, as schematically shown in Fig. 3(a). The result is shown in Fig. 3(c); (2) Extract the “bosonic spectral function” SF from $\Delta \text{Re}\Sigma(\epsilon)$ by Eq. (2), using a maximum entropy method (MEM) similar to that in Ref. [6] but with the modified integral kernel. The result is shown in Fig. 3(d). Note that the significant change of the real part of the self-energy is limited to the energy up to ~ 100 meV, above which the self-energy difference fluctuates around zero and is most likely due to the data noise, as shown in Fig. 3(c). Therefore, we assume a maximum bosonic mode energy 100 meV when doing the MEM analysis; (3) Calculate the real part of self-energy at 25K from the extracted bosonic spectral function using Eq. (1). The result is shown in Fig. 3(d); (4) Determine the bare band dispersion by taking the difference between the measured dispersion and the calculated real part of the self-energy, both at 25K. The result is shown in Fig. 3(b). These steps iterate until the result converges. We find that the procedure converges quickly and only three iterations are

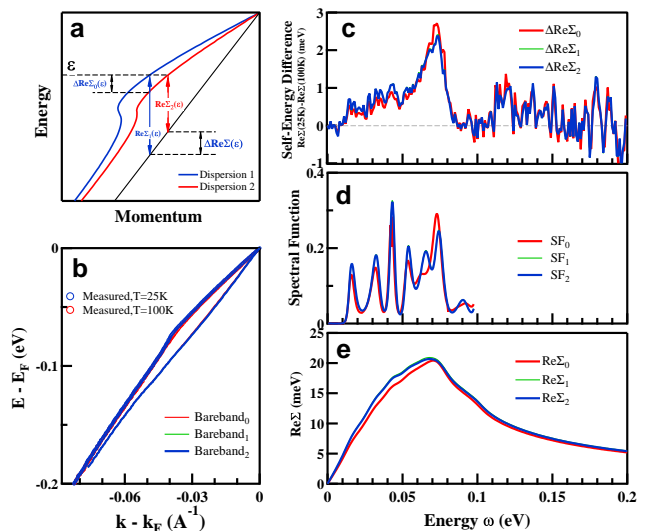


FIG. 3: Extraction procedure of the bare band and the Eliashberg spectral function. (a) Schematic plot for the two dispersions and a bare band to show the real parts of self-energies and their difference for a given energy ϵ . (b) Measured nodal dispersions of heavily overdoped Pb-Bi2201 at 25K and 100K and the extracted bare bands for different iterations. (c) Self-energy difference between the 25K and 100K dispersions for different iterations. (d) Extracted Eliashberg spectral function for different iterations. (e) Real part of electron self-energy calculated from the extracted spectral function at 25 K for different iterations.

needed for this analysis.

Fig. 4 summarizes the final results of the bare band (Fig. 4(a)), Eliashberg spectral function (Fig. 4(b)), and electron self-energy (inset of Fig. 4(a)). Although the results are obtained by using the two representative dispersions at 25K and 100K, the self-energy calculated from the extracted Eliashberg function (Fig. 4(b)) at other temperatures (here we show 60K data) matches very well with the measured values, as shown in the inset of Fig. 4(a), indicating the internal consistency of our approach. The obtained bare band is close but less steeper than the one given by the LDA calculations [27] (Fig. 4(a)), and is significantly different from the empirical one used previously (green line in Fig. 4a) [8].

Sharp features are clearly identified in the extracted Eliashberg spectral function (Fig. 4(b)). Five peaks at (14-17), (30-32), (41-44), (54-58) and (70-74) meV can be identified below 100 meV, and they are reproducible from several independent measurements. In fact, the features (14-17), (41-44) and (70-74) meV are clearly visible in the raw data (Fig. 1). These sharp features show reasonably good agreement with the phonon modes observed in the same material by infrared reflectance (Fig. 4(c)) [28] and Raman scattering (Fig. 4(d)) [29]. Note that these optical measurements only see phonon modes with zero wavevector, and the full band of phonons will exhibit dis-

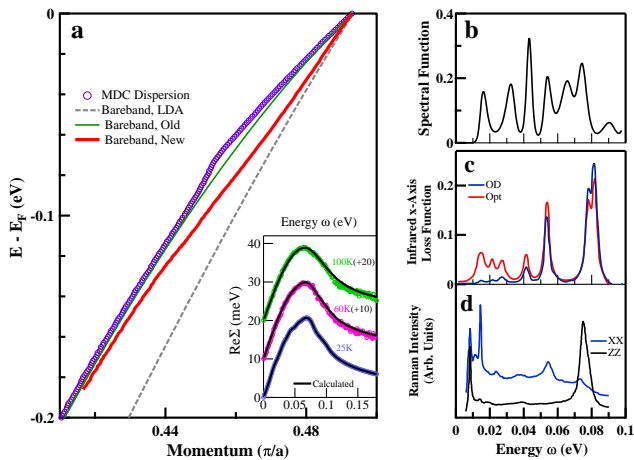


FIG. 4: Extracted bare band dispersion, self-energy and Eliashberg spectral function of heavily over-doped Pb-Bi2201. (a) Measured nodal dispersion (empty blue circles) at 25 K and the extracted bare band (thick red line). For comparison, the bare band from the band structure calculations (dashed grey line) [27] and the bare band used by previous maximum entropy method (thin green line) [27] are also shown. The bottom-right inset shows the measured electron self-energy at different temperatures and their comparison with those calculated from the extracted Eliashberg spectral function. (b) Extracted Eliashberg functions $\alpha^2 F(\omega)$. (c) Loss function from infrared measurements on optimally-doped (red line) and over-doped (blue line) Bi-2201 [28]. (d) Raman spectra of Bi2201 under different polarization geometries [29].

persion in the Brillouin zone, in particular for the higher energy phonon near 70~80 meV [30]. Considering the rather weak magnetic signal [31], and the absence of magnetic mode at 15 K for the heavily overdoped Pb-Bi2201 sample ($T_c \sim 5$ K), our present results leave no doubt that the ~ 70 meV dispersion kink is due to electron coupling with the multiple phonon modes.

With the Eliashberg function extracted, it is possible to determine quantitatively the strength of the electron-boson coupling. We calculate the mass enhancement factor $\lambda = 2 \int_0^\infty \frac{d\omega}{\omega} \alpha^2 F(\omega)$, and obtain $\lambda \approx 0.42$. As discussed above, the contribution is mainly from the electron-phonon coupling. Our study presents a conclusive evidence that the electron-phonon coupling is strong even in the heavily over-doped cuprate samples. It is much stronger than the value suggested by the first principles calculations (0.14~0.20) [23]. Our present work thus asks for a re-examination of theoretical calculations on the strength of electron-phonon coupling in these compounds.

In summary, by taking advantage of the high quality data of the laser-ARPES measurements, we have developed a new approach to determine the bare band dispersion and extract Eliashberg spectral function quantitatively. The method is general and can be applied to many other materials, thus promoting ARPES tech-

nique to be quantitative in probing many-body effects. Our results on the heavily overdoped Pb-Bi2201 demonstrate unambiguously that the ~ 70 meV nodal dispersion kink is due to electron coupling to the multiple phonons. In particular, we present a conclusive evidence that the electron-phonon coupling is strong in cuprates even in the heavily over-doped regime.

* Corresponding author: jrshi@aphy.iphy.ac.cn

† Corresponding author: XJZhou@aphy.iphy.ac.cn

- [1] G.Grimvall, *The Electron-Phonon Interaction in Metals*, edited by E.Wohlfarth (North-Holland, New York, 1981)
- [2] J. M. Rowell *et al.*, Phys. Rev. Lett.**10**, 334 (1963); D. J. Scalapino *et al.*, Phys. Rev. **148** 263 (1966)
- [3] J. F. Zasadzinski *et al.*, Phys. Rev. Lett.**96**, 017004 (2006)
- [4] S. V. Dordevic *et al.*, Phys. Rev. B.**71**, 104529 (2005); E. vanHeumen *et al.*, Phys. Rev. B.**79**, 184512 (2009)
- [5] A. Damascelli, Z. Hussain, and Z.-X. Shen, Rev. Mod. Phys. **75**, 473 (2003); J.C.Campuzano *et al.*, in *The Physics of Superconductors*, edited by K.H.Bennemann and J.B.Ketterson(Springer New York, 2004),Vol.2; X.J.Zhou *et al.*,in *Handbook of High-Temperature superconductivity: Theory and Experiment*, edited by J.R.Schrieffer(Spring,New York,2007).
- [6] J. R. Shi *et al.*, Phys. Rev. Lett.**92**, 186401(2004)
- [7] X. J. Zhou *et al.*, Phys. Rev. Lett.**95**, 117001(2005)
- [8] W. Meevasana *et al.*, Phys. Rev. Lett.**96**, 157003(2006)
- [9] M. Hengsberger *et al.*, Phys. Rev. Lett. **83**, 592 (1999)
- [10] T. Valla *et al.*, Phys. Rev. Lett. **83**, 2085 (1999)
- [11] A. Bostwick *et al.*, Nature Phys. **3**, 36(2007)
- [12] N. Mannella *et al.*, Nature(London)**438**, 474 (2005)
- [13] A. A. Kordyuk *et al.*, Phys. Rev. B.**71**, 214513 (2005)
- [14] P. V. Bogdanov *et al.*, Phys. Rev. Lett.**85**, 2581 (2000)
- [15] A. Lanzara *et al.*, Nature(London) **412**,510(2001)
- [16] P. Johnson *et al.*, Phys. Rev. Lett.**87**, 177007 (2001)
- [17] A. Kaminski *et al.*, Phys. Rev. Lett.**86**, 1070 (2001)
- [18] X. J. Zhou *et al.*, Nature(London)**423**,398(2003)
- [19] A. A. Kordyuk *et al.*, Phys. Rev. Lett.**97**, 017002 (2006)
- [20] W. T. Zhang *et al.*, Phys. Rev. Lett.**100**, 107002(2008)
- [21] T. Dahm *et al.*, Nature Phys.**5**, 217(2009).
- [22] K. Terashima *et al.*, Nature Phys.**2**, 27 (2006).
- [23] F. Giustino *et al.* Nature(London) **452**,975(2008)
- [24] R. Heid *et al.*, Phys. Rev. Lett.**100**, 137001(2008)
- [25] G. D. Liu *et al.*, Rev. Sci.Instrum. **79**, 023105 (2008).
- [26] In a real system, the "bare band" is somewhat ambiguous because the retarded effects of the electron-electron interaction could also act as the effective bosonic modes. Therefore, the "bare band" actually depends on the energy scale we are looking at. For phonon modes which usually have much smaller energy, the so called "bare band" actually already includes the renormalization effects from the other higher energy collective excitations.
- [27] W. Meevasana *et al.*,Phys. Rev. B.**75**, 174506 (2007)
- [28] A. A. Tsvekov *et al.*, Phys. Rev. B.**60**, 13196 (1999)
- [29] M. Osada *et al.*, Phys. Rev. B.**56**, 2847 (1997)
- [30] R. J. McQueeney *et al.*, Phys. Rev. Lett.**87**, 077001(2001)
- [31] S. Wakimoto *et al.*, Phys. Rev. Lett.**98**, 247003 (2007)